Charge symmetry in pion-deuteron elastic scattering

T. G. Masterson, J. J. Kraushaar, R. J. Peterson, R. S. Raymond,* R. A. Ristinen, and J. L. Ullmann
Nuclear Physics Laboratory, Department of Physics, University of Colorado, Boulder, Colorado 80309

R. L. Boudrie
Clinton P. Anderson Meson Physics Facility, Los Alamos National Laboratory, Los Alamos, New Mexico 87545

D. R. Gill
TRIUMF, Vancouver, Canada V6T 2A3

E. F. Gibson
Physics Department, California State University, Sacramento, California 95819

A. W. Thomas
Physics Department, University of Adelaide, Adelaide, South Australia, Australia
(Received 23 July 1984)

Differential cross sections for π^+d and π^-d elastic scattering have been measured and compared at 256 MeV in order to provide a sensitive test of charge symmetry in nuclear interactions. New methods for calculating external and internal Coulomb corrections are presented and compared with data at 143 and 256 MeV. Sensitivities to mass and width differences among the components of the Δ resonance are determined. Accurate absolute π^-d cross sections were measured for the first time at 256 MeV; the π^+d differential cross sections agree well with other measurements.

I. INTRODUCTION

The study of physical symmetries has fascinated man for millenia. Simplicius, circa 550 A.D., was among the first to suggest that fundamental symmetries are responsible for the construction of the physical universe. The current paper addresses the question of charge symmetry in the pion-deuteron system, one of the simplest three-body hadronic systems. Because the π^+d and π^-d systems are transformed into each other by charge symmetry, they constitute an important testing ground for this symmetry in the strong interaction. Charge symmetry breaking (CSB) effects would be observable as differences between π^+d and π^-d total or differential cross sections.

The basic pion-nucleon interaction is strongly energy dependent in the region near the 3-3 resonance. We have previously reported measurements[1] of the difference between the π^-d and π^+d differential cross sections at 143 MeV, just below the peak of the (3,3) resonance. In the present paper we report measurements made with pions at 256 MeV, just above the resonance. These two energies are also particularly interesting because they are the energies at which Pedroni *et al.*[2] at Schweizerisches Institut für Nuklearforschung (SIN) observed maximal and oppositely directed excursions from charge symmetry in $\pi^{\pm}$d total cross sections. Asymmetry measurements have also been made in the region below 100 MeV by the group at Saclay.[3] In the present work, we measured the absolute π^+d elastic differential cross sections at 256 MeV; these agree well with the existing data of Gabathuler *et al.*[4] The present work is the first accurate measurement of π^-d elastic cross sections in this energy region.

At a beam energy of 143 MeV, where the greatest difference between π^-d and π^+d total cross sections was found,[2] our earlier data for the angular dependence of the asymmetry showed a deviation from charge symmetry caused by Coulomb effects, a residual difference after the removal of Coulomb effects, and some evidence of unexpected structure near 100 deg. The residual CSB effect was modeled by breaking charge symmetry for the πN interaction through the mass differences among the four charge states of the delta, the first excited state of the nucleon. Since, in the energy region studied here, the πN interaction is largely mediated by this resonance, this loss of symmetry produces an angle- and beam energy-dependent difference in the $\pi^{\pm}$d cross sections.

On the higher energy side of the 3-3 resonance the total cross sections for π^+d and π^-d again differ,[2] showing a broad extremum in the difference near a pion laboratory energy of 250 MeV. With the change in the sign of the real part of the πN amplitude relative to that below the resonance, another view of charge symmetry breakdown in that resonance could be expected.

We report here measurements of the differential cross section asymmetry, A_π, for laboratory angles between 18 and 115 deg for elastic pion-deuteron scattering at 256 MeV. The experimental methods are described in Sec. II.

The extraction of CSB information from the asymmetry data requires careful treatment of both external and internal Coulomb corrections. In Sec. III we present a detailed treatment of external Coulomb corrections, including relativistic effects. These calculations are compared with our data at both 143 and 256 MeV. They are also compared with our previous less detailed calculations at

143 MeV and with the calculations of Fröhlich *et al.*[5]

Internal Coulomb corrections are those which in principle violate charge symmetry, such as the mass differences between the neutron and proton and among the components of the Δ isobar. The effect of these Coulomb corrections is examined in Sec. III and compared with the recent calculations of Rinat and Alexander.[6] Finally, we examine the effect of combined calculations of both external and internal Coulomb corrections on the pion asymmetry data at both 143 and 256 MeV and show the sensitivity of this combined analysis to mass and width differences among the members of the Δ isobar.

II. EXPERIMENTAL PROCEDURES

The experiment was performed at the Energetic Pion Channel and Spectrometer (EPICS) facility of the Clinton P. Anderson Meson Physics Facility (LAMPF). The experimental procedures were very similar to those described in some detail for previous $\pi^{\pm}$d elastic scattering measurements[1] carried out with pions of 143 MeV. The major experimental difference between this work and the previous work was that an evacuated coupling between the spectrometer and the scattering chamber was in place for the 256 MeV experiment. This eliminated possible effects due to scattering in the vacuum windows. The basic method employed was to take data on targets of CD_2, CH_2, and C at one angular setting of the spectrometer for both π^- and π^+ using the known $\pi^{\pm}$p cross sections for absolute normalization of the data.

The mean incident pion energy in the present work was 256 MeV (370 MeV/c). The data of Pedroni *et al.*[2] on total pion-deuteron cross sections indicated a larger deviation from charge symmetry at this energy than at any other pion energy above the (3,3) resonance. This energy also provides an excellent check on possible systematic errors in the earlier work at 143 MeV because the sign of the deviation from charge symmetry is expected to be reversed at 256 MeV. In addition, there exist excellent normalization data from π^+p elastic scattering at 236 and 264 MeV, and from π^-p scattering at 238 and 264 MeV. These data are reported by Bussey *et al.*[7] Differential cross section data have been taken at SIN by Gabathuler *et al.*[4] for π^+d at 256 MeV. Measurements[8–10] of the vector polarization, iT_{11}, have suggested anomalous fluctuations at this energy, and similar anomalous fluctuations have been reported for the tensor polarization, T_{20}, by some observers[11,12] but not by others.[13]

The full momentum acceptance of the channel (±1%) was used for all π^+ and π^- data runs. Except for sign reversal, channel settings were identical for both pion polarities. The data were taken in three run periods spread over an interval of several months. Each pion asymmetry data point, requiring π^+ and π^- data for each target at a specific angle, included only data taken immediately adjacent to each other in time in order to eliminate any possible long term systematic fluctuations. During these run periods the proton production beam current was in the range of 450–650 μA and the corresponding pion fluxes were in the range of $1.8-2.6\times10^8$ pions/sec for π^+ and $2.2-3.2\times10^7$ pions/sec for π^-. Within each run period proton beams and pion fluxes were constant to within approximately 10%.

The pion flux was monitored with two ion chambers in the pion beam approximately 0.7 m downstream from the scattering target; the primary proton beam was monitored just upstream from the production target by recording pulses induced in a toroid through which the beam passes. The ion chambers were located inside the evacuated scattering chamber. A 4.5 cm thick carbon absorber between the ion chambers stopped the protons in the π^+ beam. All flux monitors agreed within 1%. At the smallest scattering angle the ion chambers interfered with the scattered beam and were moved to the side. These short runs were taken with only the primary proton beam current monitor to determine the pion flux.

Because, at least at lower energies, the pion fraction of the beam through the channel is known[1] to depend on the position of the proton beam on the production target, this position was carefully monitored through the course of the experiment by use of harp scans taken every few hours. Typical variations were no greater than 0.3 mm, corresponding to no more than 0.5% variation in the pion fraction.[1] Absolute cross section determinations are independent of pion fraction and of differences between μ^+ and μ^- content in the beam. They are very slightly dependent on a relative change in muon content between data and normalization runs. At 256 MeV the muon content of the beam on target was less than 8%.

The scattering targets were CD_2 (194 mg/cm^2), CH_2 (145 or 292 mg/cm^2), and C (131 or 302 mg/cm^2). The isotopic purity of the deuterium target was greater than 99%. The nominal beam spot size was 10 cm×20 cm and the target size was approximately 15 cm×23 cm. Mean scattering energies are listed in Table I for each angle. Because differential pion absorption between the CD_2 and CH_2 targets could possibly affect the relative ion chamber readings for the two sets of data, absorption corrections were made. These corrections, based on the data of Richard-Serre *et al.*,[14] were less than 0.1% and thus negligible.

TABLE I. Differential cross sections for $\pi^{\pm}$p elastic scattering used in the analysis of the $\pi^{\pm}$d data at 256 MeV. The values listed with their uncertainties were calculated using the SCATPI (Ref. 15) program.

θ_{lab}	$T_{\pi mean}$ (MeV)	π^+p $\frac{d\sigma}{d\Omega}$ (mb/sr)	π^-p $\frac{d\sigma}{\delta\Omega}$ (mb/sr)
18.5	255.82	35.05 ±0.23	2.963 ±0.040[a]
26.2	255.90	28.68 ±0.16	2.705 ±0.035
32.0	255.70	23.91 ±0.11	2.420 ±0.030
39.0	255.70	18.45 ±0.08	2.022 ±0.025
45.0	255.65	14.346±0.067	1.681 ±0.021
52.5	255.64	10.066±0.054	1.287 ±0.016
60.0	255.75	6.903±0.043	0.967 ±0.012
66.5	255.60	5.028±0.036	0.7615±0.0093
90.0	255.55	3.001±0.021	0.5315±0.0082
105.0	255.50	3.579±0.022	0.6253±0.0085

[a]The mean energy for this measurement was 255.64 MeV.

Data were obtained over laboratory angles ranging from 18 to 115 deg. The forward angle was limited by high rates in the wire chambers due to forward scattered protons and the largest angle was near the large-angle limit of the spectrometer. The angular resolution of the spectrometer was 0.5 deg, limited by the angular convergence of the incident beam in the scattering plane. Absolute scattering angles could be set within 0.1 deg.

Scattered pions were detected with the spectrometer and data acquisition system of EPICS. Each pion through the spectrometer had its trajectory defined by a series of delay-line drift chambers. A full kinematic calculation was done and the missing mass histogrammed for each event through the spectrometer. A typical FWHM resolution was 600 keV, mostly due to reaction kinematics. Pions were identified by the usual software projections. Pions decaying between the target and spectrometer produced a small and continuous background which canceled out exactly in the $\pi^{\pm}$d ratios.

As in the earlier experiment at 143 MeV, all magnets were cycled between polarity changes and the dipole magnet fields were set to an accuracy of 1 part in 10^4 by use of a nuclear magnetic resonance (NMR) gaussmeter. The exact reversal of all magnetic fields without any other experimental configuration changes, and the temporal juxtaposition of π^+ and π^- data collection reduced many systematic uncertainties and effects of possible long-term fluctuations. Data collected with the carbon target enabled background subtraction for both the CD_2 and CH_2 targets. Background subtraction was accomplished both by normalizing to the ion chamber readings and by equating areas in the exclusively carbon scattering regions of the spectra. The two methods were consistent.

The data were normalized with the $\pi^{\pm}$p differential cross sections calculated with the SCATPI phase shift code,[15] based on the $\pi^{\pm}$p phase shifts determined by Carter, Bugg, and Carter.[16] This set of phase shifts is strongly influenced by the accurate data of Bussey *et al.*[7] and was determined by independent fitting of π^+p and π^-p data, thus explicitly allowing charge-dependent phase shifts. In the present determination of πd cross sections, the largest uncertainty is in the calculated πp cross sections used for normalization. These cross sections are listed in Table I; if other data become available, one could adjust the analysis accordingly. The present absolute πd cross section determinations are the best possible with normalization information available at this time. The choice of the SCATPI cross sections over those predicted by other sets of phase shifts was made for reasons outlined in our earlier work.[1] In short, the SCATPI approach produced the best agreement with measured differential cross sections.

Differential cross sections for both π^+d and π^-d are shown in Figs. 1 and 2, respectively, and tabulated in Table II. Also included in Fig. 1 are the π^+d differential cross sections measured by Gabathuler *et al.*[4] at 256 MeV and the back angle data of Stanovnik *et al.*[17] The agreement with our data is very good. The data are also compared to the three-body calculations of Rinat and Thomas.[18]

The ratio of the difference between π^-d and π^+d cross sections to the sum is called the asymmetry, A_π, and is the parameter used to describe deviations from charge symmetry. The ratio measurement is far more precise than the individual cross section measurements as many uncertainties cancel in the ratio. In particular, uncertainties due to target thickness, pion decay, dead time corrections, and count rate effects are essentially eliminated in the ratio.

The asymmetry data are shown in Fig. 3. These data are corrected for radiative effects following the prescrip-

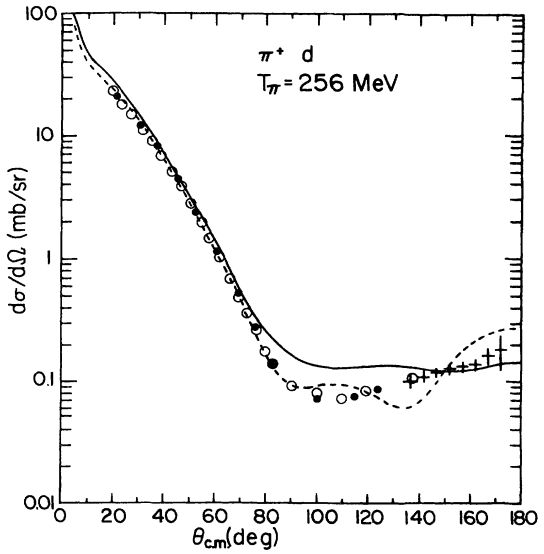

FIG. 1. Differential cross sections for π^+d elastic scattering at 256 MeV. Solid circles represent the present work, open circles that of Gabathuler *et al.* (Ref. 4), and crosses that of Stanovnik *et al.* (Ref. 17) (at 260 MeV). The solid line is a calculation based on the theoretical pion-deuteron amplitudes of Rinat and Thomas (Ref. 18) while the dashed line is the result of a phase shift fit by Arvieux (Ref. 31).

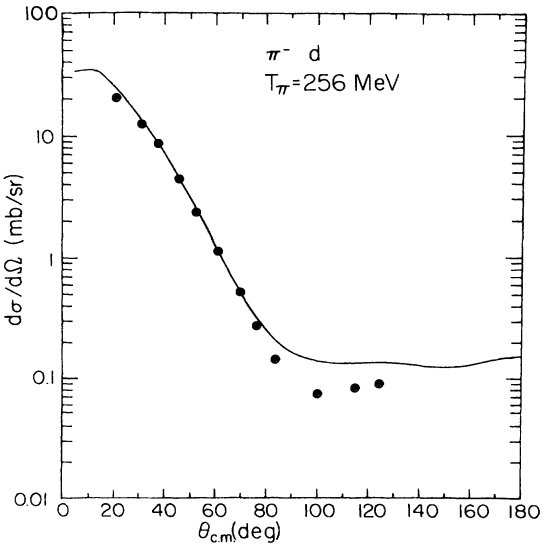

FIG. 2. Measured differential cross sections for π^-d elastic scattering at 256 MeV. The curve is calculated with the theoretical πd amplitudes of Rinat and Thomas (Ref. 18).

TABLE II. Measured $\pi^{\pm}$d differential cross sections and asymmetry ratios for $\pi^{\pm}$d elastic scattering at 256 MeV. Radiative corrections are included in all values listed in this table.

$\theta_{c.m.}$ (deg)	c.m. cross sections $d\sigma/d\Omega$ (mb/sr)[a] π^+d	π^-d	A_π[b]
22.01	20.97 ±0.25	20.37 ±0.44	−0.014±0.012
	21.22 ±0.50	20.53 ±0.90	−0.017±0.025
31.08	12.90 ±0.17	12.99 ±0.28	0.003±0.013
	11.75 ±0.18	12.57 ±0.30	0.033±0.014
37.81	8.20 ±0.10	8.28 ±0.18	0.003±0.013
45.92	4.48 ±0.05	4.40 ±0.09	−0.012±0.012
52.69	2.52 ±0.04	2.50 ±0.05	−0.006±0.012
	2.27 ±0.03	2.36 ±0.04	0.017±0.010
61.06	1.17 ±0.01	1.16 ±0.02	−0.008±0.011
69.24	0.532±0.007	0.536±0.011	−0.000±0.013
76.23	0.270±0.005	0.273±0.006	0.002±0.015
83.06	0.138±0.003	0.145±0.004	0.018±0.017
100.29	0.076±0.002	0.081±0.003	0.026±0.020
	0.070±0.001	0.073±0.003	0.014±0.020
114.75	0.076±0.002	0.084±0.002	0.037±0.018
124.04	0.087±0.002	0.092±0.003	0.021±0.019

[a]Differential cross section errors include all statistical errors in πd and πp measurements as well as πp systematic errors calculated by SCATPI.

[b]Asymmetry ratio errors include πd statistical errors, πp systematic errors, and errors from the ratio of πp yield to $\sigma_{\pi p}$ (SCATPI) (Ref. 15).

tion given by Borie.[19] These corrections have been applied both to $\pi^{\pm}$p and to $\pi^{\pm}$d systems. The former correction is somewhat larger since the $\pi^{\pm}$p system is lighter. The net effect of these corrections on A_π is small, less than 0.01, as given in Table III. It would have been possible to apply a slightly more accurate radiative correction described by Fröhlich *et al.*,[5] but the further effect on A_π would have been less than 0.001. Other than the radiative correction, no further corrections have been made to the data in Fig. 3. The errors shown include both statistics in the data and uncertainties (see Table I) in the $\pi^{\pm}$p cross sections. Four of the data points (22, 31, 53, and 100 deg) are the weighted averages of repeated measurements.

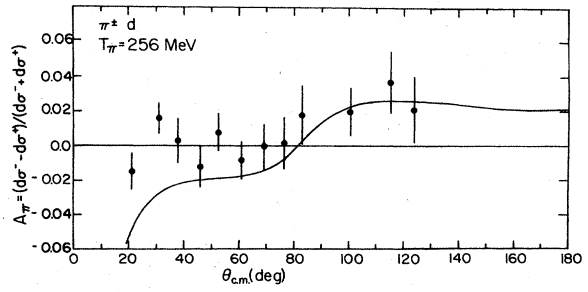

FIG. 3. Asymmetry measurements at 256 MeV. Radiative corrections are included in the data shown. The curve includes corrections due to Coulomb amplitudes and the interference of Coulomb and nuclear amplitudes only, and is the starting point for calculations of other external and internal Coulomb corrections.

III. THEORY

The pion-deuteron system is relatively well described by a three-body approach.[18,20–30] These calculations include all pion-nucleon S and P partial waves, a realistic description of the deuteron, off-diagonal t-matrix elements, true pion absorption, and relativistic kinematics. There is impressively good agreement between theory and differential cross section data[1] at 143 MeV, but all calculations still overestimate the region of the cross section minimum at 256 MeV as shown in Figs. 1 and 2. Arvieux has also

TABLE III. Radiative corrections for the $\pi^{\pm}$d and $\pi^{\pm}$p differential cross sections and asymmetry ratios. The corrections were calculated from equations from Borie (Ref. 19). The corrections are included in the data listed in Table II.

$\theta_{c.m.}$ (deg)	Radiative corrections (mb/sr) π^-d	π^-p	π^+d	π^+p	Corrections to A_π
22.01	0.006	0.006	0.005	0.004	−0.001
31.08	0.010	0.011	0.009	0.007	−0.001
37.81	0.015	0.015	0.012	0.010	−0.001
45.92	0.020	0.020	0.016	0.013	−0.002
52.69	0.024	0.025	0.019	0.015	−0.002
61.06	0.029	0.031	0.022	0.017	−0.003
69.24	0.034	0.037	0.025	0.019	−0.004
76.23	0.039	0.042	0.028	0.021	−0.005
83.06	0.045	0.045	0.031	0.021	−0.005
100.29	0.052	0.058	0.034	0.023	−0.008
114.75	0.059	0.067	0.036	0.023	−0.010
124.04	0.062	0.065	0.038	0.023	−0.009

made a phase shift fit[31] to π^+d data starting from various theoretical sets of phase shifts; this fit is shown in Fig. 1.

A. Coulomb corrections

The theoretical πd phase shifts of Rinat and Thomas[18] provide the basis for our calculation of Coulomb corrections and our examination of charge symmetry breaking effects. It has been shown[1] that a perfect description of the πd differential cross section is not needed to extract Coulomb corrections and CSB effects since the theoretical cross section difference, $\sigma(\pi^-\mathrm{d})-\sigma(\pi^+\mathrm{d})$, is essentially model independent. If there were no Coulomb contribution and CS were strictly valid, the asymmetry parameter,

$$A_\pi=[d\sigma^-(\theta)-d\sigma^+(\theta)]/[d\sigma^-(\theta)+d\sigma^+(\theta)]\ ,$$

would be zero.

The πd scattering amplitude can be represented as a sum of Coulomb and nuclear parts:

$$f(\theta)=f_C(\theta)+f_N(\theta)\ . \tag{1}$$

To test charge symmetry, the Coulomb contributions to $f(\theta)$ must be removed. In order to put external and internal Coulomb corrections into context, let us look diagramatically at πN and πd scattering. Pion-nucleon scattering is dominated by the coupling to a "bare" Δ three-quark state. The actual Δ has width and a slight shift in position due to coupling to the πN system and self-energy due to successive recombinations, as shown in Fig. 4, where $M_\Delta^{(0)}$ is the bare Δ mass and $\Sigma_{\pi N}$ is the Δ self-energy. The self-energy term typically involves the exchange of a 500–600 MeV virtual pion and is relatively small, making a perturbation theory approach possible.

The diagrams for the π^+d interaction, including Coulomb effects, are shown in Fig. 5. Here, terms 1, 2, and iterations correspond to the strong πd scattering for which we use the three-body amplitudes of Ref. 18 which, at 256 MeV, are fully relativistic three-body amplitudes for πd scattering with no true absorption and 6.7% deuteron D state. Terms 3, 4, and iterations correspond to pure Coulomb scattering, and have been calculated as in Ref. 1 starting from the same three-body amplitudes. The resulting curve is shown in Fig. 3, and is a starting point for further calculations. A similar approach has been taken by Fröhlich *et al.*[5] (see the following text). Terms 5–8 are external Coulomb corrections and will be discussed in Secs. III B (nonrelativistically) and III C (relativistically).

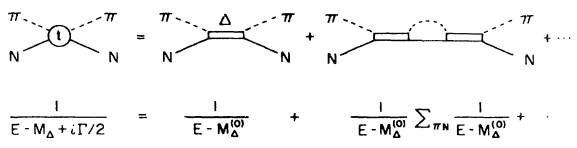

FIG. 4. Graphs for pion-nucleon scattering.

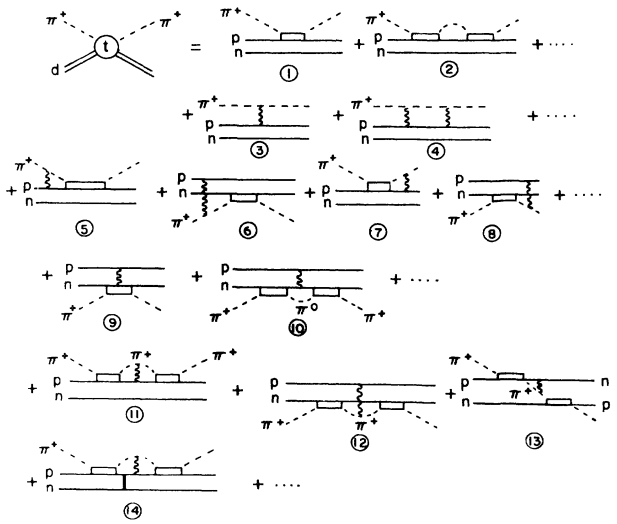

FIG. 5. Graphs for π^+d scattering, including Coulomb effects. See the text for an explanation of each term.

Terms 9–12 and 14 are "internal" Coulomb corrections and will be discussed in Sec. III D. Finally, term 13 is a true three-body internal Coulomb correction which has yet to be estimated.

B. External Coulomb corrections to πd scattering

The nuclear amplitude

$$f_N(\theta)=\sum_l(2l+1)e^{2i(\sigma_l-\sigma_0)}\left[\frac{e^{i\delta_l}\sin\delta_l}{k}\right]P_l(\cos\theta) \tag{2}$$

involves Coulomb contributions both through the Coulomb phases σ_l,

$$\sigma_l=\arg\Gamma(l+1+i\eta)\ , \tag{3}$$

(where η is the Sommerfeld parameter $=Ze^2/\hbar v$) and through the phase shifts δ_l,

$$\delta_l=\delta_l^N+\delta_l^{fs}+\delta_l^{CN}\ . \tag{4}$$

Here δ_l^N is the pure three-body πd phase shift without any Coulomb effects, δ_l^{fs} is the correction to the point Coulomb phase shift (σ_l) due to the charge distribution in the deuteron and is approximated by multiplying $f_C(\theta)$ by the deuteron form factor $F(q/2)$, and δ_l^{CN} arises from the quantum mechanical interference between Coulomb and nuclear potentials. An exact evaluation of δ_l^{CN} requires a full solution to the three-body Coulomb-nuclear problem, which is not presently possible.

Previously,[1] we estimated δ_l^{CN} by evaluating the three-body πd amplitudes $f_l=(e^{i\delta_l}\sin\delta_l)/k$ at an energy differing from the incident energy by ±0.75 MeV. A Breit-Wigner form for the τ matrix ($=e^{i\delta_l}\sin\delta_l$) was assumed and the change in the τ matrix for each partial wave was given by

$$\frac{\Delta\tau_l}{\Delta E_l}=\left[\frac{2}{\Gamma_{\rm el}^{(l)}}\tau_l(E)+\frac{(3+a^2k^2)}{(1+a^2k^2)}\frac{\omega_k}{k^2}\times\left[1+i\frac{\Gamma^{(l)}}{\Gamma_{\rm el}^{(l)}}\tau_l(E)\right]\right]\tau_l(E)\ , \tag{5}$$

where $\Gamma_{\rm el}^{(l)}$ is the elastic πd width in the lth partial wave; Γ^l is the total πd width; a is 1.15 fm; k is the pion momentum in the πd c.m. system (k is 1.08 fm^{-1} at 143 MeV and 1.56 fm^{-1} at 256 MeV); and $\omega_k^2=k^2+m_\pi^2$. Fröhlich *et al.*[32] give a nonrelativistic on-shell approximation for $\delta_l^{\rm CN}$,

$$\delta_l^{\rm CN}=\tfrac{1}{2}\tan^{-1}\left[\frac{\alpha_l{\rm Im}\zeta}{1+\alpha_l{\rm Re}\zeta}\right], \tag{6}$$

where

$$\zeta=2i\delta'_{s,l}(p)+\frac{(1-e^{-2i\delta_{s,l}(p)})}{p}\ , \tag{7}$$

and where the coefficients α_l are given by:

$$\alpha_l=\frac{2\mu e^2}{\pi}{\rm P}\int_0^\infty dx\frac{x}{1-x^2}Q_l\left[\frac{1+x^2}{2x}\right]=-\frac{\mu e^2}{C_l}\ , \tag{8}$$

where P denotes the principal value, Q_l is the associated Legendre function of the second kind, and μ is the reduced mass. The $\delta_l^{\rm CN}$ obtained in this manner are purely real, an impossibly stringent assumption on $\delta_l^{\rm CN}$.

Haftel and Zankel[33] have obtained a complete form for $\delta_l^{\rm CN}$ which they derived independently from the original assumptions of Fröhlich *et al.*[32]

$$\tan\delta_l^{\rm CN}=\frac{-\eta k}{C_l}\left[\delta'_{s,l}+\frac{\sin2\delta_{s,l}}{2k}\right]. \tag{9}$$

For small values of $\delta_l^{\rm CN}$ this reduces to

$${\rm Re}\delta_l^{\rm CN}=\frac{-\eta k}{C_l}\left[{\rm Re}\delta'_{s,l}+\frac{\sin(2\,{\rm Re}\delta_{s,l})\cosh(2\,{\rm Im}\delta_{s,l})}{2k}\right], \tag{10}$$

$${\rm Im}\delta_l^{\rm CN}=\frac{-\eta k}{C_l}\left[{\rm Im}\delta'_{s,l}+\frac{\cos(2\,{\rm Re}\delta_{s,l})\sinh(2\,{\rm Im}\delta_{s,l})}{2k}\right]. \tag{11}$$

Here C_l is related to the above-mentioned α_l by

$$\frac{1}{C_l}=-\frac{\alpha_l}{\mu e^2}$$

and the values of C_l are the same as before and are tabulated in Table VI.

The phase shifts $\delta_l^{\rm CN}$ determined by these relationships now must be related to phase shifts in the πd amplitudes f_{lj}. The relationship is

$$f_{lj}=\frac{1}{2k}[\sin(2\,{\rm Re}\delta_{lj})e^{-2\,{\rm Im}\delta_{lj}}]+\frac{i}{2k}[1-\cos(2\,{\rm Re}\delta_{lj})e^{-2\,{\rm Im}\delta_{lj}}]\ , \tag{12}$$

TABLE IV. Amplitudes and phase shifts calculated at 256 MeV from Rinat and Thomas (Ref. 18) three-body πd amplitudes with 6.7% deuteron D state and no absorption.

l	j	Ref_{lj}	Imf_{lj}	Reδ_{lj}	Imδ_{lj}
1	0	−0.062 54	0.090 74	−7.613	8.511
1	1	−0.098 03	0.127 21	−13.446	11.208
0	1	−0.137 20	0.169 70	−21.147	12.960
2	1	−0.033 50	0.035 04	−3.346	3.121
2	2	−0.071 60	0.103 47	−9.129	9.688
1	2	−0.125 03	0.254 41	−31.067	23.438
3	2	−0.013 97	0.017 54	−1.320	1.582
3	3	−0.030 23	0.048 73	−3.173	4.548
2	3	−0.068 28	0.125 58	−9.652	12.588
4	3	−0.007 20	0.008 14	−0.660	0.729
4	4	−0.009 98	0.019 40	−0.949	1.773
3	4	−0.029 95	0.053 08	−3.195	5.008
5	4	−0.001 92	0.003 47	−0.173	0.311
5	5	−0.004 36	0.008 22	−0.400	0.742
4	5	−0.016 01	0.021 13	−1.531	1.913
6	5	−0.000 91	0.001 61	−0.082	0.144
6	6	−0.002 05	0.003 00	−0.185	0.269
5	6	−0.004 75	0.009 04	−0.437	0.816
7	6	−0.000 41	0.000 72	−0.038	0.064
7	7	−0.000 97	0.001 45	−0.087	0.130
6	7	−0.002 27	0.004 05	−0.205	0.364
7	8	−0.001 00	0.001 83	−0.090	0.164

or, inversely

$${\rm Re}\delta_{lj}=\tfrac{1}{2}\tan^{-1}\left[\frac{{\rm Re}f_{lj}}{\frac{1}{2k}-{\rm Im}f_{lj}}\right], \tag{13}$$

$${\rm Im}\delta_{lj}=\tfrac{1}{2}\ln\left[\frac{\sin(2\,{\rm Re}\delta_{lj})}{2k\,{\rm Re}f_{lj}}\right]. \tag{14}$$

Table IV gives the Rinat and Thomas[18] 256 MeV πd amplitudes and phase shifts. The τ matrix may be expressed in a Breit-Wigner resonant form

$$\tau_l=e^{i\delta_l}\sin\delta_l=\frac{\Gamma_{\rm el}^{(l)}}{2(E_R^{(l)}-E)-i\Gamma^{(l)}}\ , \tag{15}$$

where $E_R^{(l)}$ is the resonant energy of the lth partial wave. E is the incident pion energy in the laboratory and the widths Γ are energy dependent:

$$\Gamma(k)=\Gamma_0\frac{k^3}{k_0^3}\left[\frac{1+k_0^2a^2}{1+k^2a^2}\right], \tag{16}$$

where k is the πd c.m. momentum and k_0 is the momentum resulting from decay at rest. The derivative of the τ matrix with respect to kinetic energy E is

$$\frac{d\tau_l}{dE}=\left[\frac{2\tau_l}{\Gamma_{\rm el}^{(l)}}+\frac{(3+a^2k^2)}{(1+a^2k^2)}\frac{\omega_k}{k^2}\left[1+i\frac{\Gamma^{(l)}}{\Gamma_{\rm el}^{(l)}}\tau_l\right]\right]\tau_l\ . \tag{5}$$

To obtain the derivative of the phase shift we start with $\tau=e^{i\delta}\sin\delta$ and obtain $d\tau/dp=\tau(i+\cot\delta)\delta'$. The derivative of the phase shift δ with respect to momentum is then given by

TABLE V. Partial wave resonant energies from the πd phase-shift analysis of Arvieux (Ref. 31).

l	j	E_R (MeV)
1	1	180
0	1	160
2	1	217[a]
1	2	210
3	2	210[a]
2	3	217
3	4	200

[a] E_R values from the present work.

$$\delta_l' = \frac{d\delta_l}{dp} = \left[\frac{2\tau_l}{\Gamma_{\rm el}^{(l)}} + \left(\frac{3+a^2k^2}{1+a^2k^2} \right) \frac{\omega_k}{k^2} \left(1 + i \frac{\Gamma^{(l)}}{\Gamma_{\rm el}^{(l)}} \tau_l \right) \right] \times \frac{p}{E+m} \frac{1}{(i+\cot\delta_l)} \,. \quad (17)$$

Finally, we need values of E_R, Γ_l, and Γ. The E_R values have been obtained from the πd phase shift analysis of Arvieux,[31] as shown in Table V. The resonance energies for all other partial waves were assumed to be 200 MeV. Contributions from all other partial waves were small (1–5 %), except for the P_0, D_2, and F_3 waves for which the contributions were 10–25 % that of the largest partial wave, the P_2 wave.

Total and elastic widths from any set of πd amplitudes were obtained using the resonant energies and the relationships

$$\Gamma = 2(E_R - E)/\zeta \quad (18)$$

and

$$\Gamma_l = \Gamma(1+\zeta^2)\mathrm{Im}\tau \,, \quad (19)$$

where $\zeta = \mathrm{Re}\tau/\mathrm{Im}\tau$.

We can now calculate the phase shift $\delta_l^{\rm CN}$ due to the quantum mechanical interference of Coulomb and nuclear potentials given by Eqs. (10) and (11). These complex phase shifts must be subtracted from or added to the three-body phase shift given by Eqs. (13) and (14) for π^+d or π^-d scattering. Using Eq. (12) to regenerate the complex amplitudes f_{lj}, we can then obtain $\pi^\pm$d cross sections [using Eqs. (1) and (2)] which should agree with experimental data if there were no charge symmetry violating effects.

The solid line in Fig. 3 is the 256 MeV asymmetry ratio A_π, including only simple external Coulomb effects due to pure Coulomb and interference of Coulomb and strong amplitudes.

The effects of various changes in the theoretical treatment of the Coulomb-nuclear interference at 256 MeV are shown in Fig. 6. The long dashed curve is the full nonrelativistic approach of Haftel and Zankel[33] and includes in the external Coulomb correction both the derivative and nonderivative terms of Eqs. (10) and (11). We also investigated the effect of turning off the second terms in Eqs. (10) and (11), terms which should be present even if the derivatives of the phase shift, $\delta_l'(p)$, were zero. The dotted-dashed curve includes only the derivative term and differs significantly from the long-dashed curve, indicating the importance of including both terms at this energy. For the short dashed curve, the location of the mean energy of the $l=1$, $j=0$ partial wave is changed from 200 to 160 MeV. This decomposition of the resonance was used only to translate t matrices to phase shifts and back, and the values are taken from the axis-crossing points of the Argand diagrams in the phase shift analysis of Arvieux[31] (see Table V). The value of the resonant energy for the $l=1$, $j=0$ partial wave is somewhat uncertain but is probably less than 200 MeV. The short and long dashed curves are almost identical, indicating the insensitivity of the analysis at 256 MeV to the resonant energy of this partial wave. Relativistic effects are, however, important and these are discussed in the following.

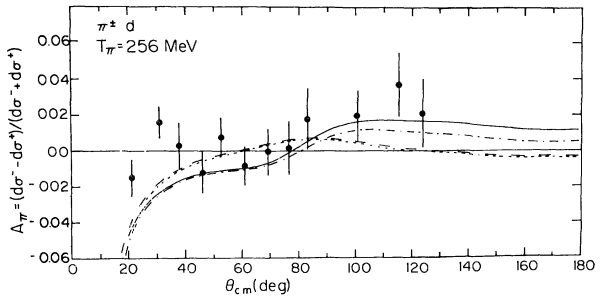

FIG. 6. External Coulomb corrections to πd asymmetry calculations at 256 MeV. The long-dashed curve is the full nonrelativistic calculation of Haftel and Zankel (Ref. 33), the dotted-dashed curve includes only the derivative term (see the text), the short-dashed curve shows the effect of changing the P_0 partial wave resonant energy from 200 to 160 MeV, and the solid curve includes relativistic effects.

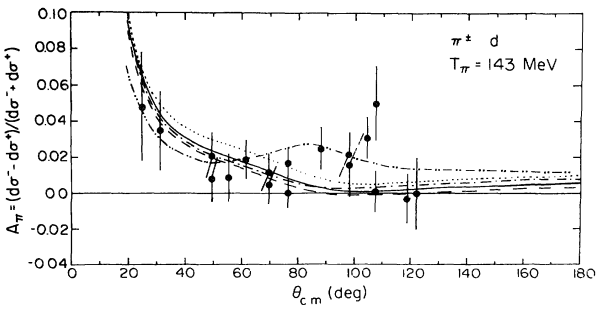

FIG. 7. External Coulomb corrections to πd asymmetry calculations at 143 MeV. The long-dashed curve is the full nonrelativistic calculation of Haftel and Zankel (Ref. 33), the dotted-dashed curve includes only the derivative term (see the text), the short-dashed curve shows the effect of changing the P_0 partial wave resonant energy from 200 to 160 MeV, the solid curve includes relativistic effects, and the dotted-dotted-dashed curve shows the effect of the relativistic extended particle treatment of Fröhlich *et al.* (Ref. 5).

The effects of similar changes in the theoretical treatment of Coulomb-nuclear interference at 143 MeV are shown in Fig. 7. The long-dashed curve corresponds to the full nonrelativistic treatment of Haftel and Zankel[33] and includes both derivative and nonderivative Coulomb correction terms, while the dotted-dashed curve includes the derivative term only. These curves are almost identical, indicating the insensitivity of the analysis at 143 MeV to this additional term, and indicating that its inclusion would not change any conclusions from our previous analysis[1] at that energy. The long-dashed curve uses a nominal value of 200 MeV for the $l=1$, $j=0$ pion deuteron partial wave, while the short-dashed curve uses a value of 160 MeV. This latter value is much closer to the incident energy in the Breit-Wigner parametrization of the resonance for this partial wave, and this variation produces a significant change in the external Coulomb correction. This is perhaps an indication that the best parametrization at this energy is the overall one used in the previous 143 MeV analysis or that a better partial wave resonance energy is needed here. As at 256 MeV, relativistic effects are important and are discussed below.

A comparison may be made between the treatment of external Coulomb corrections given here and that of Fröhlich *et al.*[5] Their concurrent and independent treatment of external Coulomb corrections is very thorough and in most respects similar to ours. We make no attempt to duplicate their analysis but point out two minor differences. Their expression for the derivative of the phase shift [(cf. Eq. (17)] is somewhat simpler than our expressions as we explicitly include the energy dependence of the derivative of the τ matrix. This effect is more important at higher energies as shown above. In one instance (their case "*e*"), they use a pion-deuteron amplitude which differs slightly from ours. The effect is to modify the point Coulomb phases σ_l to "relativistic extended particle" Coulomb phases. This introduces a small bump in the 143 MeV calculation near 90° and is shown as the dotted-dotted-dashed curve in Fig. 7. This is particularly interesting in that our 143 data[1] exhibit a small bump in this angular region, a bump which could not be described in the context of the theory we presented.

C. External Coulomb corrections to $\pi^{\pm}$d scattering (relativistic)

The use of a nonrelativistic approximation for Coulomb corrections to pion scattering in the 100–300 MeV region is somewhat questionable. The Blankenbecler-Sugar formalism has been used by Fröhlich and Zankel[34] to obtain a relativistic relationship for the external Coulomb phase shift.

Incorporating their results into the relationships of Haftel and Zankel,[33] we obtain

$$\mathrm{Re}\delta_l^{\mathrm{CN}}=\frac{-\eta k}{C_l}\left[\mathrm{Re}\delta'_{s,l}+\frac{\sin(2\,\mathrm{Re}\delta_{s,l})\cosh(2\,\mathrm{Im}\delta_{s,l})}{2k}\left[1+\frac{p^2}{E_1E_2}\right]\right] \tag{20}$$

and

$$\mathrm{Im}\delta_l^{\mathrm{CN}}=\frac{-\eta k}{C_l}\left[\mathrm{Im}\delta'_{s,l}+\frac{\cos(2\,\mathrm{Re}\delta_{s,l})\sinh(2\,\mathrm{Im}\delta_{s,l})}{2k}\left[1+\frac{p^2}{E_1E_2}\right]\right], \tag{21}$$

where $E_1=\sqrt{p^2+m_\pi^2}$, $E_2=\sqrt{p_2+m_{\mathrm{d}}^2}$, and p is the c.m. momentum of the pion. The values of C_l are now given by

$$C_l=\frac{\pi}{2}\frac{1}{I_{\mathrm{rel}}}, \tag{22}$$

where

$$I_{\mathrm{rel}}=\sqrt{S}\,\mathrm{P}\int_0^\infty dp' Q_l\left[\frac{p^2+p'^2}{2pp'}\right]\frac{p'(E'_1+E'_2)}{2E'_1E'_2[S-(E'_1+E'_2)^2]} \tag{23}$$

and $S=(E_1+E_2)^2$.

This integral is nonanalytic and involves the Legendre functions Q_l of the second kind; these have an infinite series of poles at $p'=p$. The integral was evaluated by transforming to a dimensionless form, translating the starting point to -1 (to move the singularities to the origin), and reflecting the $(-1,0)$ part of the integral about the origin to effect a near cancellation of the singularities. Different representations of the hypergeometric functions involved in Q_l were required for regions near to and far from the origin in order to perform the integrations in a finite amount of computer time. The adaptive quadrature integration routine of Lyness[35] was used to perform the integrations. The original calculations of Fröhlich *et al.*[32] for the nonrelativistic coefficients C_l were reproduced with this code and the relativistic coefficients C_l were determined for $T_\pi=143$ and 256 MeV. All coefficients are tabulated in Table VI. As expected for pions of these energies, the relativistic corrections were significant.

The relativistic Coulomb prediction at 256 MeV is shown as the solid curve in Fig. 6. This introduces a structure into the external Coulomb calculation closely resembling the trend of the experimental data. The relativistic external Coulomb calculation at 143 MeV is shown as the solid curve in Fig. 7. Differences between this curve and the analogous nonrelativistic curve (long-dashed) are small, indicating the relativistic effects are less important at 143 MeV.

D. Internal Coulomb corrections

We consider next the effect of internal Coulomb or charge symmetry violating corrections on the calculated

TABLE VI. Coefficients C_l for calculating Coulomb corrections.

	Nonrelativistic (energy independent)	Relativistic 143 MeV	Relativistic 256 MeV
C_0	0.6366	1.104 89	1.208 39
C_1	1.5708	2.5084	2.7333
C_2	2.5465	4.0057	4.3659
C_3	3.5343	5.5338	6.0343
C_4	4.5272	7.0744	7.7170
C_5	5.5224	8.6213	9.4066
C_6	6.5191	10.1716	11.0998
C_7	7.5174	11.7240	12.7953
C_8	8.5149	13.2779	14.4923
C_9	9.5134	14.8328	16.1903

asymmetry A_π. These are due to mass and width differences among the components of the delta isobar as well as to the neutron-proton mass difference. We will also explicitly include the deuteron spin.

Internal Coulomb corrections are shown diagrammatically as terms 9—14 in Fig. 5. Term 9 represents the Δ self-energy, $\Sigma_{\pi N}$. For the π^+d interaction, it corresponds to an upward shift in the effective Δ^+ mass (in the π^+n interaction) of $\langle V_c \rangle \sim 0.7$ MeV. For the π^-d interaction it corresponds to a downward shift in the effective Δ^- mass (in the π^-n interaction) of $-\langle V_c \rangle \sim -0.7$ MeV. This term is the largest correction considered here and corresponds to Eq. (13) in the internal Coulomb corrections of Rinat and Alexander.[6]

The graphs 10—12 in Fig. 5 correspond to changes in the Δ self-energy $\Sigma_{\pi N}$. Since $\Sigma_{\pi N}$ is of the order of 100 MeV, and the correction is of the order $[\langle V_c \rangle/(\text{virtual point energy})] \times (\Delta \text{ self-energy}) \approx (0.7/600) \times 100 \approx 0.1$ MeV, these corrections are too small to have a significant effect here. Graph 13 in Fig. 5 is a true three-body correction which has yet to be estimated. It would, however, act in the same direction as graph 9. Graph 14 also acts in the same direction as graph 9 but is a small correction (claimed to be fourth order by Rinat and Alexander[6]) and is not included here.

In order to determine the magnitude of these effects we write the pion deuteron scattering amplitude in impulse approximation as

$$f_{\pi d}(\theta) = [f_{\pi p}(\theta) + f_{\pi n}(\theta)] F_d(\theta) , \tag{24}$$

where $f_{\pi N}$ is the pion nucleon scattering amplitude and $F_d(\theta)$ is the deuteron form factor. Following the analysis of Ref. 1 we can write the pion nucleon scattering amplitudes as sums of charge-symmetry-conserving isospin $\frac{3}{2}$ and $\frac{1}{2}$ amplitudes and charge symmetry violating amplitudes ϵ:

$$\begin{aligned}
&\pi^+\text{p}: \ f_{\pi^+\text{p}} = f_{3/2} + \epsilon_{++} , \\
&\pi^+\text{n}: \ f_{\pi^+\text{n}} = (f_{3/2} + 2f_{1/2} + \epsilon_{+-})/3 , \\
&\pi^-\text{p}: \ f_{\pi^-\text{p}} = (f_{3/2} + 2f_{1/2} + \epsilon_{-+})/3 , \\
&\pi^-\text{n}: \ f_{\pi^-\text{n}} = f_{3/2} + \epsilon_{--} .
\end{aligned} \tag{25}$$

The charge symmetry violating component of the cross section can then be evaluated,[1] including deuteron spin, as

$$\Delta\sigma = \frac{3}{8\Gamma_t} \text{Re} \left[\{ [f^*_{3/2}(\text{NF}) + \tfrac{1}{2} f^*_{1/2}(\text{NF})] \mathcal{F} \} \begin{pmatrix} 2\cos\theta \\ k \end{pmatrix} + \tfrac{2}{3} [(f^*_{3/2}(\text{F}) + \tfrac{1}{2} f^*_{1/2}(\text{F}) \mathcal{F}] \begin{pmatrix} -\sin\theta \\ k \end{pmatrix} \right] , \tag{26}$$

where NF and F refer to non-spin-flip and spin-flip terms and

$$\mathcal{F} = f_{0_t} [\tilde{C}_{\Gamma_t} + f_{0_t} (i\tilde{C}_{\Gamma_t} - 2C_w)] . \tag{27}$$

The C_w and $\tilde{C}_\Gamma$ terms give the mass and width differences among the components of the delta:

$$C_w = W_{--} - W_{++} + (W_{-+} W_{+-})/3 , \tag{28}$$

$$\tilde{C}_\Gamma = \Gamma_{--} - \Gamma_{++} + (\Gamma_{-+} - \Gamma_{+-})/3 , \tag{29}$$

(as originally defined by Pedroni *et al.*[2]), where the subscripts $--$, $-+$, $+-$, and $++$ refer to the Δ^-, Δ^0, Δ^+, and Δ^{++}, respectively, and are related to ϵ_{ij} by

$$\epsilon_{--} - \epsilon_{++} + (\epsilon_{-+} - \epsilon_{+-})/3 = f_{0_t} [\tilde{C}_\Gamma + f_{0_t} (\tilde{C}_{\Gamma_t} - 2C_w)]/\Gamma_t . \tag{30}$$

The neutron-proton mass difference is incorporated into C_w by writing

$$C_w^{\text{eff}} = C_w - 2(M_n - M_p)/3 .$$

The Δ self-energy term (term 9 previously mentioned) enters in exactly the same way as the mass shift of the Δ [Eq. (28)]: $\langle V_c \rangle_{\Delta^-} - \langle V_c \rangle_{\Delta^+}/3$. Thus the effective value of C_w becomes

$$\begin{aligned}
C_w^{\text{eff}'} &= C_w - 2(M_n - M_p)/3 - 4\langle V_c \rangle/3 \\
&= C_w - 1.9 \text{ MeV} ,
\end{aligned} \tag{31}$$

since $\langle V_c \rangle$ is 0.7 MeV. The incorporation of terms 13 and 14 into this relationship would further reduce the value of C_w^{eff}, and thus our C_w value must be regarded as a lower bound.

This difference reduces C_w by about 1.9 MeV and is included in all calculations. Only values of C_w, not C_w^{eff}, will be quoted to facilitate comparison with other C_w determinations. The relativistic Breit-Wigner amplitude f_{0_t} is given by

$$f_{0_t} = \frac{W_0 \Gamma_t}{(W_0^2 - W^2) - i W_0 \Gamma_t} , \tag{32}$$

where W is the total energy. The widths Γ are also energy dependent:

$$\Gamma_i = \Gamma_{0_i} \left(\frac{k}{k_{0_i}} \right)^3 \left(\frac{1 + k_{0_i}^2 a^2}{1 + k^2 a^2} \right) , \tag{33}$$

where k is the pion-nucleon c.m. momentum and $a = 1.15$ fm.

All terms $f_{\pi N}$, $\tilde{C}_\Gamma$, and Γ are evaluated at the appropriate pion-nucleon subenergy (about 10 MeV less than the pion-deuteron c.m. energy) to optimize the three-body impulse approximation. This is equivalent to the "G_f" approximation of Rinat and Alexander,[6] whereas the use of the πd c.m. energy would be equivalent to their "G_e" approximation.

The cross section difference [Eq. (26)] is in the pion-nucleon c.m. system. It is transformed to the pion-deuteron c.m. system by

$$\cos\theta_{\pi N}=\frac{(\alpha^2+\beta^2)\cos\theta_{\pi d}-2\alpha\beta}{\alpha^2+\beta^2-2\alpha\beta\cos\theta_{\pi d}}\ , \tag{34}$$

where

$$\alpha=\frac{m+\omega/2}{m+\omega}\ \text{and}\ \beta=\frac{\omega}{2(m+\omega)}\ .$$

In Fig. 8 the sensitivity of the theoretical A_π calculations at 256 MeV to the mass splitting parameter, C_w, is shown. The solid curve is the base value—the relativistic curve of Fig. 6—to which the internal Coulomb corrections were applied. For all curves in this figure the value of $\tilde{C}_\Gamma$ was 2.33 MeV as calculated from Eqs. (29) and (33). The dotted-dashed curve corresponds to $C_w=0$, the dotted curve to $C_w=2.0$ MeV, the dashed curve to $C_w=4.47$ MeV (the bag model value of Bickerstaff and Thomas[36]), and the dotted-dotted-dashed curve to $C_w=6.6$ MeV (the value used by Rinat and Alexander[6]). Values from 2 to 4.5 MeV agree with the data.

The same sensitivity to the C_w parameter is shown in Fig. 9 for calculations made at 143 MeV. For all curves in this figure the value of $\tilde{C}_\Gamma$ was 1.24 MeV as calculated from Eqs. (29) and (33). Again, the solid curve is the relativistic curve from Fig. 7 and corrections were applied to this curve. The dotted-dashed curve corresponds to $C_w=0$, the dotted curve to $C_w=2$ MeV, the dashed curve to $C_w=4.47$ MeV (bag model[36]), and the dotted-dotted-dashed curve to $C_w=6.6$ MeV (Rinat and Alexander[6]). The analysis at this energy is more sensitive to the value of C_w and only values from 2 to 4 MeV are consistent with the data.

In Fig. 10 the sensitivity of the theoretical A_π calculation at 256 MeV to the width parameter $\tilde{C}_\Gamma$ is shown. In Fig. 10(a) the mass splitting parameter, C_w, is 0 MeV,

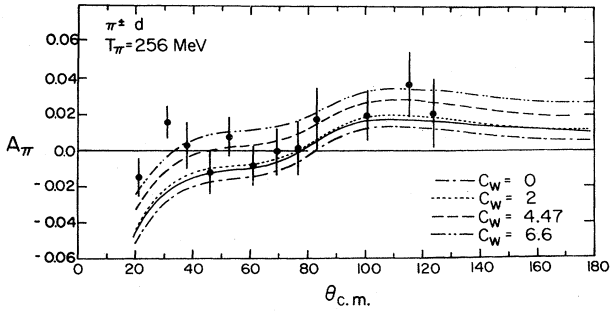

FIG. 8. Effect of changes in the mass splitting parameter C_w on A_π asymmetry calculations at 256 MeV. For all curves shown here, the energy dependent width parameter $\tilde{C}_\Gamma$ was set to its calculated value of 2.33 MeV.

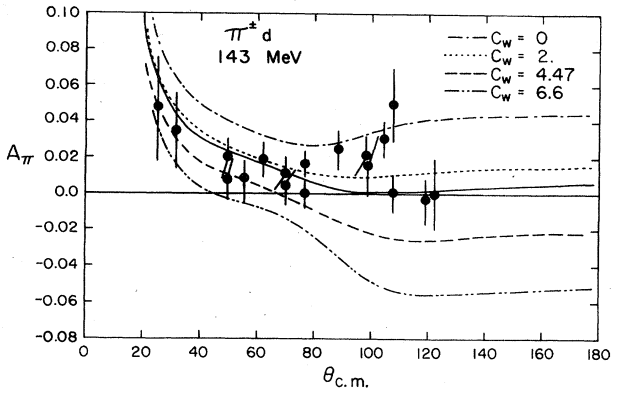

FIG. 9. Effect of changes in the mass-splitting parameter C_w on A_π asymmetry calculations at 143 MeV. The energy dependent width parameter $\tilde{C}_\Gamma$ was fixed at its calculated value of 1.24 MeV.

while in Fig. 10(b), $C_w=4.47$ MeV. The solid curve is, as in the other figures, the relativistic curve from Fig. 6 and corrections are applied to this. The dotted-dashed curves correspond to $\tilde{C}_\Gamma=0$, the dashed curves correspond to the calculated $\tilde{C}_\Gamma$ value of 2.33 MeV, and the dotted curves to $\tilde{C}_\Gamma=3.6$, the value obtained by Pedroni *et al.*[2] Differences among these three curves are too small to suggest any preference, as a larger effect comes from changing the value of C_w, as seen in Fig. 8.

In Fig. 11 the sensitivity of theoretical A_π calculations at 143 MeV to the width parameter $\tilde{C}_\Gamma$ is shown. The solid curve corresponds again to the relativistic calculation of Fig. 7 and corrections were applied to this curve.

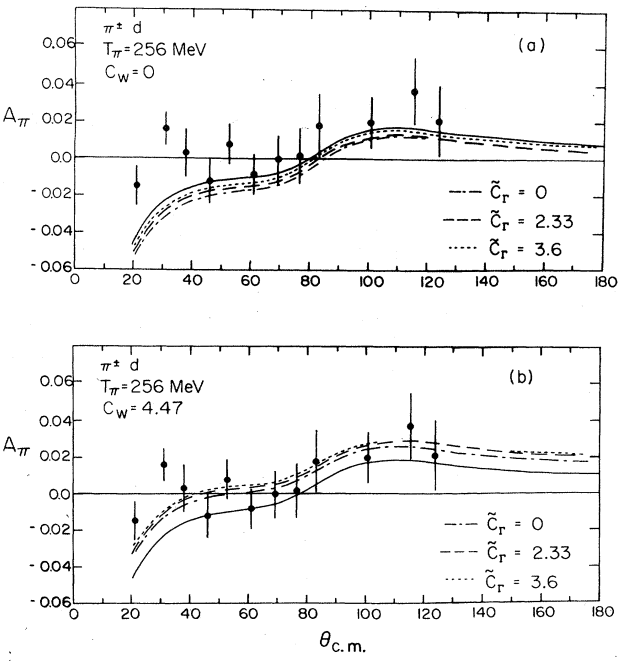

FIG. 10. Sensitivity of A_π asymmetry calculations to the value of the width parameter $\tilde{C}_\Gamma$ at 256 MeV, using two values of C_w.

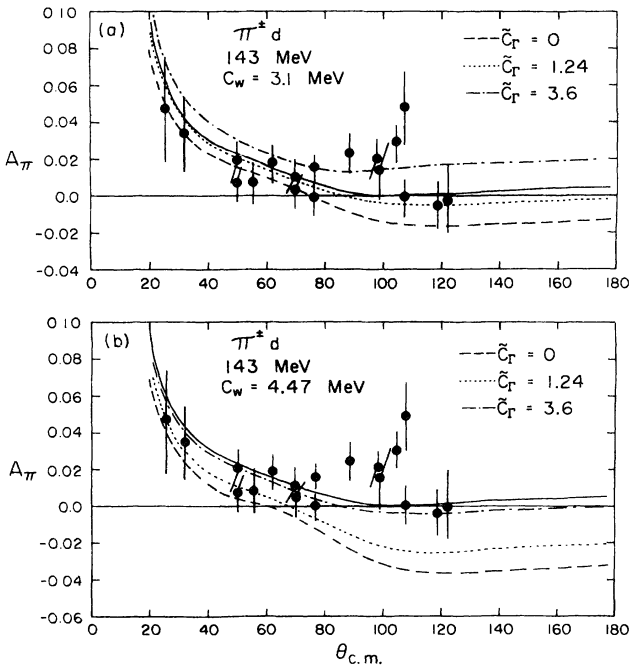

FIG. 11. Sensitivity of A_π asymmetry calculations to the value of the width parameter $\tilde{C}_\Gamma$ at 143 MeV, using the two values of C_w.

The dashed curve corresponds to $\tilde{C}_\Gamma=0$ MeV, the dotted curve to the calculated value of $\tilde{C}_\Gamma=1.24$ MeV, and the dotted-dashed curve to the energy independent value of 3.6 MeV for $\tilde{C}_\Gamma$ obtained by Pedroni *et al.*[2] The calculations at 143 MeV are sensitive to both C_w and $\tilde{C}_\Gamma$. In Fig. 11(a), where $C_w=3.1$ MeV, values of $\tilde{C}_\Gamma$ from 0 to 1.5 MeV agree well with the data. In Fig. 11(b), where $C_w=4.47$ MeV, a larger value of $\tilde{C}_\Gamma$ from 3 to 4 MeV would be required to agree with the data.

A two-parameter fit indicates a correlation between C_w and $\tilde{C}_\Gamma$ values with $\Delta\tilde{C}_\Gamma=\frac{4}{3}\Delta C_w$ giving the same χ^2 at 143 MeV. At 256 MeV there is essentially no sensitivity to $\tilde{C}_\Gamma$. We have therefore made determinations with calculated $\tilde{C}_\Gamma$ values. At 143 MeV, we find $C_w=3.1\pm1$ MeV, and at 256 MeV $C_w=4.5\pm1.3$ MeV. The 143 MeV analysis omitted the data points in the bump near 100° which is not described by the theory described here. Inclusion of all data points would lower the 143 MeV value for C_w by about 1 MeV. An external Coulomb correction similar to case "*e*" described by Fröhlich *et al.*[5] could give a better description of this structure but would not change the value of C_w from that found by disregarding the structure in this small angular region. One must remember here, however, that uncertainties in the fundamental πN phase shifts could alter the values of C_w.

IV. CONCLUSIONS

We have measured $\pi^{\pm}$d differential cross sections at 256 MeV. Our π^+d differential cross sections are in good agreement with previous measurements of Gabathuler *et al.*[4] Our π^-d differential cross sections are the first accurate π^- measurements in this energy region.

Absolute cross sections were obtained by measuring $\pi^{\pm}$p differential cross sections and normalizing to known $\pi^{\pm}$p differential cross sections based on the phase shift analysis of Carter, Bugg, and Carter,[16] the only charge independent phase shift analysis available. Both $\pi^{\pm}$p and $\pi^{\pm}$d differential cross sections are tabulated so that the present theoretical analysis could be repeated if better $\pi^{\pm}$p cross sections were to become available.

Our most accurate experimental measurements are of the pion symmetry A_π, shown in Fig. 3; the data include small radiative corrections. Many experimental uncertainties cancel, and even uncertainties due to $\pi^{\pm}$p phase shift analysis are reduced in this ratio.

The pion asymmetry differs from zero because of external and internal (charge symmetry breaking) Coulomb effects, and this paper contains the first theoretical analysis including both. The necessary corrections are shown diagrammatically in Fig. 5. This analysis is applied both to our present data at 256 MeV and to our previous data[1] at 143 MeV. Our theoretical analysis is based on the three-body hadronic πd amplitudes of Rinat and Thomas.[18]

External Coulomb corrections are made for pure Coulomb, Coulomb-nuclear interference, and finite deuteron size effects. Our theoretical analysis of these corrections is considerably more detailed than our previous treatment, with the inclusion of relativistic effects and a nonderivative term in the Coulomb-nuclear interference phase shift. Our analysis is similar to the independent analysis of external Coulomb corrections by Fröhlich *et al.*[5] A particular feature of their analysis is the "relativistic extended particle" Coulomb phase shift which introduces a bump in the A_π calculation near 90° at 143 MeV. A similar structure was observed in our 143 MeV data.[1] This feature, affecting only the 80°–100° region, has not been included in our analysis and does not change the values of the mass or width parameters presented here. The effects of our external Coulomb corrections are shown in Figs. 6 and 7 for 256 and 143 MeV, respectively.

Our internal Coulomb corrections include effects due to mass differences between the neutron and the proton, mass and width differences among the intermediate Δ isobar, and the Δ's self-energy. Our analysis is also compared with the internal Coulomb corrections of Rinat and Alexander.[6] The effects of mass differences are contained in the C_w parameter and width differences in the $\tilde{C}_\Gamma$ parameter. Effects due to C_w variations are shown in Figs. 8 and 9, while effects due to $\tilde{C}_\Gamma$ variation are shown in Figs. 10 and 11 for the 256 and 143 MeV analysis, respectively. Our analyses favor values of C_w between 2.0 and 4.5 MeV and the energy dependent calculated value for $\tilde{C}_\Gamma$. More restrictive limits on C_w and $\tilde{C}_\Gamma$ must await better charge independent $\pi^{\pm}$p phase shifts. The 143 MeV analysis is more sensitive to small changes in these CSB parameters, and back angle (120°–180°) $\pi^{\pm}$ asymmetry data would be very useful here.

ACKNOWLEDGMENTS

We would like to thank the staff of LAMPF for experimental and computational support, and C. Eime for help with data analysis. This work was supported in part by the U. S. Department of Energy.

*Present address: University of Michigan Group, Brookhaven National Laboratory, Upton, NY 11973.
[1]T. G. Masterson *et al.,* Phys. Rev. C **26**, 2091 (1982).
[2]E. Pedroni *et al.,* Nucl. Phys. **A300**, 321 (1978).
[3]B. Balestri *et al.,* Nucl. Phys. **A392**, 217 (1983).
[4]K. Gabathuler *et al.,* Nucl. Phys. **A350**, 253 (1980).
[5]J. Fröhlich, B. Saghai, C. Fayard, and G. H. Lamot, Saclay Report No. 2121-12/1983, 1983.
[6]A. S. Rinat and Y. Alexander, Nucl. Phys. **A404**, 467 (1983).
[7]P. J. Bussey *et al.,* Nucl. Phys. **B58**, 363 (1973).
[8]J. Bolger *et al.,* Phys. Rev. Lett. **46**, 167 (1981).
[9]J. Bolger *et al.,* Phys. Rev. Lett. **48**, 1667 (1982).
[10]G. R. Smith *et al.*, Phys. Rev. C **29**, 2206 (1984).
[11]J. Ulbricht *et al.,* Phys. Rev. Lett. **48**, 311 (1982).
[12]W. Gruebler *et al.,* Phys. Rev. Lett. **49**, 444 (1982).
[13]R. J. Holt *et al.,* Phys. Rev. Lett. **43**, 1229 (1979); **47**, 472 (1981).
[14]C. Richard-Serre *et al.,* Nucl. Phys. **B20**, 413 (1970).
[15]SCATPI, a subroutine for calculating πN cross sections and polarizations for incident pion energies between 90 and 300 MeV, J. B. Walter and G. A. Rebka, Los Alamos Report UC34A, 1979 (unpublished).
[16]J. R. Carter, D. V. Bugg, and A. A. Carter, Nucl. Phys. **B58**, 378 (1973).
[17]A. Stanovnik *et al.,* Phys. Lett. **94B**, 323 (1980).
[18]A. S. Rinat and A. W. Thomas, Nucl. Phys. **A282**, 365 (1977); and private communication.
[19]E. Borie, Phys. Lett. **68B**, 433 (1977).
[20]L. D. Faddeev, Zh. Eksp. Teor. Fiz. **39**, 1459 (1960) [Sov. Phys.—JETP **12**, 1014 (1961)].
[21]N. M. Petrov and V. V. Peresypkin, Phys. Lett. **44B**, 321 (1973).
[22]A. W. Thomas and I. R. Afnan, Phys. Lett. **45B**, 437 (1973).
[23]F. Myhrer, Nucl. Phys. **B80**, 491 (1974).
[24]G. D. Doolen, Ph.D. thesis, Purdue University, 1968.
[25]F. Myhrer and D. S. Koltun, Nucl. Phys. **B86**, 441 (1975); F. Myhrer, *ibid.* **A241**, 524 (1975).
[26]N. Giraud, Y. Avishai, C. Fayard, and G. H. Lamot, Phys. Rev. C **19**, 465 (1979).
[27]A. S. Rinat, Y. Starkand, E. Hammel, and A. W. Thomas, Phys. Lett. **80B**, 166 (1979).
[28]C. Fayard, G. H. Lamot, and T. Mizutani, Phys. Rev. Lett. **45**, 524 (1980).
[29]K. Kubodera, M. P. Locher, F. Myhrer, and A. W. Thomas, J. Phys. G **6**, 171 (1980).
[30]J. R. Afnan and B. Blankleider, Phys. Rev. C **22**, 1638 (1980).
[31]J. Arvieux, Phys. Lett. **103B**, 99 (1981); J. Arvieux and A. S. Rinat, Nucl. Phys. **A350**, 205 (1980); and private communication.
[32]J. Fröhlich, L. Streit, H. Zankel, and H. Zingl, J. Phys. G **6**, 841 (1980).
[33]M. I. Haftel and H. Zankel, Phys. Rev. C **24**, 1322 (1981).
[34]J. Fröhlich and H. Zankel, in *Proceedings on Few Body Systems and Nuclear Forces, Graz, 1978,* edited by H. Zingl, M. Haftel, and H. Zankel (Springer, Berlin, 1978), p. 113.
[35]J. N. Lyness, Commun. ACM **13**, 260 (1970), algorithm 379.
[36]S. Théberge, A. W. Thomas, and G. A. Miller, Phys. Rev. D **22**, 2838 (1980), **23**, 2106(E) (1981); A. W. Thomas, Adv. Nucl. Phys. **13**, 1 (1984); R. P. Bickerstaff and A. W. Thomas, Phys. Rev. D **25**, 1861 (1982); J. A. Niskanen, Phys. Lett. **107B**, 344 (1981).